

# **Gravitational microlensing and the finite dimensions of the stars**

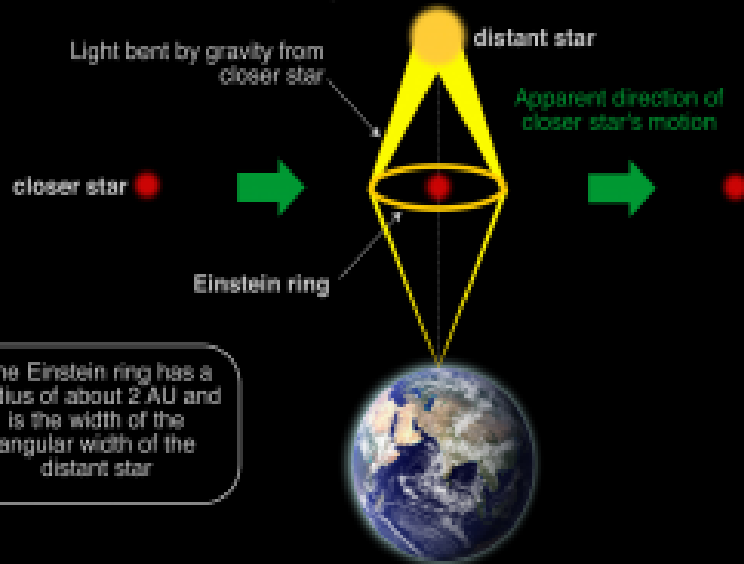
**Dr. Lindita Hamolli**

**Department of Physics, Tirana University, Albania**

**International Workshop on LHC, Astrophysics, Medical and  
Environmental Physics. Shkodra (Albania), 6-8 October 2014**

# Gravitational microlensing

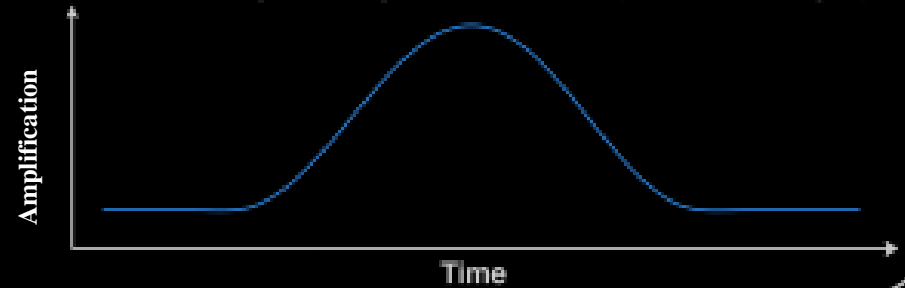
The Earth, a close star, and a brighter, more distant star, happen to come into alignment for a few weeks or months



Gravity from the closer star acts as a lens and magnifies the distant star over the course of the transit.



The change in brightness can be plotted on a graph



$$R_E(M, D_L) = D_L \sqrt{\frac{4GM}{c^2} \frac{D_{LS}}{D_L D_S}}$$

$$T_E = \frac{R_E(M, D_L)}{v_T}$$

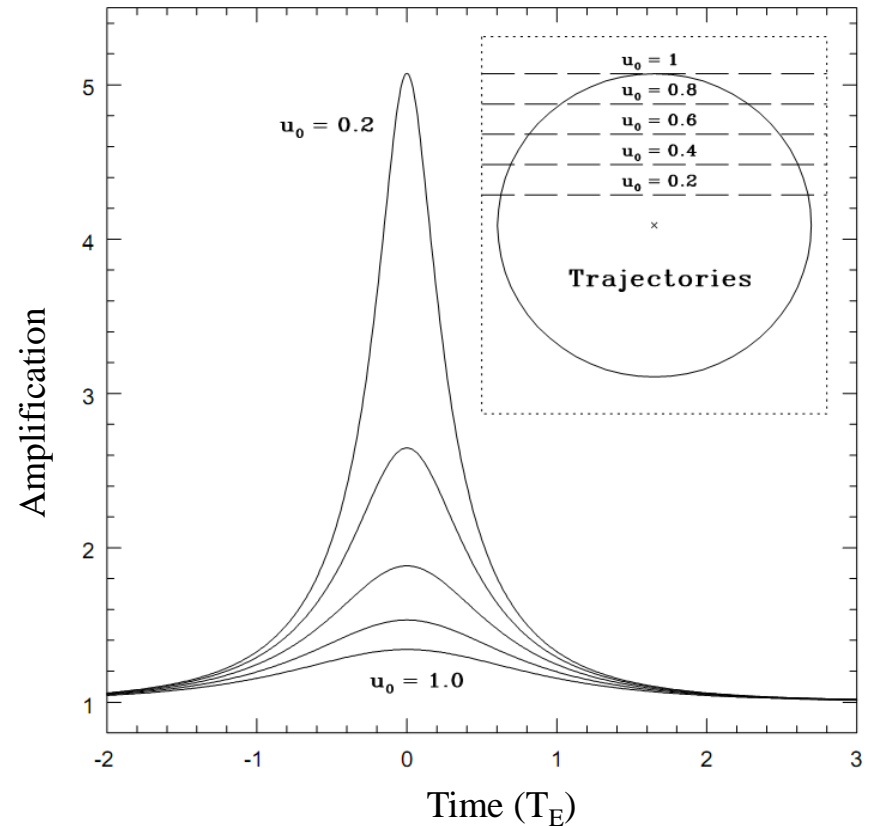
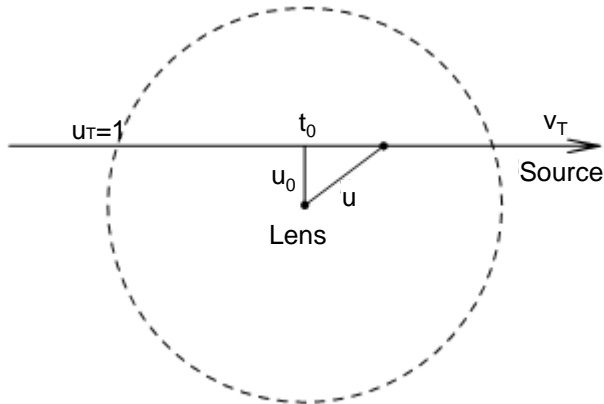
$$A(u) = \frac{u^2(t) + 2}{u(t) \sqrt{u^2(t) + 4}}$$

# Gravitational microlensing

Measurable parameters are:  $u_0$ ,  $t_0$ ,  $T_E$

$$u(A) = \sqrt{2} \left[ \left( \frac{A^2}{A^2 - 1} \right)^{1/2} - 1 \right]^{1/2}$$

$$u(t) = \sqrt{u_0^2 + \left( \frac{t - t_0}{T_E} \right)^2}$$



# Gravitational microlensing

## Anomalies in the light curves

- Parallax effect
- Binary lens
- Finite source effects

# The limb-darkening coefficients (LDC) laws by the stellar atmosphere models

- Linear  $I(\mu) = I(1)[1 - U(1 - \mu)]$
- Quadratic  $I(\mu) = I(1)[1 - a(1 - \mu) - b(1 - \mu)^2]$
- Square root  $I(\mu) = I(1)[1 - c(1 - \mu) - d(1 - \sqrt{\mu})]$
- Logarithmic  $I(\mu) = I(1)[1 - e(1 - \mu) - f \mu \ln \mu]$
- **New non-linear**  $I(\mu) = I(1)[1 - a_1(1 - \mu^{1/2}) - a_2(1 - \mu) - a_3(1 - \mu^{3/2}) - a_4(1 - \mu^2)]$

$\mu = \cos(\theta)$ , where  $\theta$  is the angle between the line of sight and the emergent intensity.

The last law describe the specific intensity at any part of the disk, better than the others

# Free-floating planets (FFPs)

- **Population of objects with  $M < 0.01 M_{\text{J}}$**

Direct observations in Sigma Orionis and Taurus  
Gravitational microlensing towards Galactic Bulge

- **Unbound to a host star or very distant (over 100 AU)**
- **Their origin is uncertain**

Believed that these objects may have formed in proto-planetary disks and subsequently scattered into unbound or very distant orbits, becoming FFPs.

- **The gravitational microlensing, is the only way, to detect these objects at distances larger than a few tens of parsecs.**

# EUCLID Mission (2018)

- Gravitational microlensing observations for 10 months
- Euclid will observe towards the Galactic center ( $l = 1.1^\circ$ ,  $b = -1.7^\circ$ )
- Field of view is  $0.54 \text{ deg}^2$
- Cadence is 20 min
- The threshold amplification  $A_{\text{th}} = 1.001$ .
- The photometric error, 0.1%

# Mass function of FFPs

Sumi et al. 2011 by the detailed analysis of the MOA-II 2006-2007 data and from the statistical investigation of the event timescale distribution revealed a significant excess of events with  $t < 2$  days, compared to prediction.

For stars and brown dwarfs they consider a power-law mass function continuous in overall interval of masses.

$$\frac{dN}{dM} \propto M^{-\alpha} = \begin{cases} \alpha = 2 & \text{for } 0.7M_s < M < M_s \\ \alpha = 1.3 & \text{for } 0.08M_s < M < 0.7M_s \\ \alpha_{BD} = 0.49^{+0.24}_{-0.27} & \text{for } 0.01M_s < M < 0.08M_s \end{cases}$$

They proposed with a high confidence level the power-law mass function for FFPs

$$\frac{dN}{dM} = k_{PL} M^{-\alpha_{PL}} \quad \alpha_{PL} = 1.3^{+0.3}_{-0.4} \quad 10^{-5} M_s < M < 10^{-2} M_s$$



# Spatial distribution of FFPs

For free-floating planets we considerate two models:

a) triaxial bulge with mass density given by

$$\rho(M, x, y, z) = \rho_0(M) e^{-s^2/2} \quad s^4 = \left(\frac{x^2}{a^2} + \frac{y^2}{b^2}\right)^2 + \frac{z^4}{c^4}$$

$$a = 1.49 \text{ kpc}$$

$$b = 0.58 \text{ kpc}$$

$$c = 0.40 \text{ kpc}$$

b) double exponential disk with mass density given by

$$\rho(M, R, z) = \rho_0(M) e^{-|z|/H} e^{-(R-R_0)/h}$$

with parameters for thin components

$$R_0 = 8.5 \text{ kpc}$$

$$h = 3.5 \text{ kpc}$$

$$H = 300 \text{ pc}$$

with parameters for thick components

$$R_0 = 8.5 \text{ kpc}$$

$$h = 3.5 \text{ kpc}$$

$$H = 1000 \text{ pc}$$

# Velocity distribution of FFPs

We assume that the velocity distribution follow a Maxwellian form (Han & Gould)

$$f(v_i) \propto \exp\left[-\frac{(v_i - \bar{v}_i)^2}{2\sigma_i^2}\right] \quad i \in \{x, y, z\}$$

Bulge  $\bar{v}_z = \bar{v}_y = 0 \quad \sigma_z = \sigma_y = 100 \text{ km/s}$

Thin disk  $\bar{v}_z = 0 \quad \bar{v}_y = 220 \text{ km/s} \quad \sigma_z = \sigma_y = 30 \text{ km/s}$

Thick disk  $\bar{v}_z = 0 \quad \bar{v}_y = 220 \text{ km/s} \quad \sigma_z = \sigma_y = 50 \text{ km/s}$

# Finite source effects

In microlensing events, in which,  $u_0 \gtrsim \rho_*$ , the point-source approximation is not valid anymore. In these events, the lens may pass over a source disk, providing a chance to measure:

- **The limb-darkening profile of a remote source,**
- **The angular Einstein radius of the lens**  $\theta_E = \frac{R_E}{D_L}$

# Finite source effects

When the lens pass over the source disk, at the moment of the entrance (exit) of the lens into (from) the source disk, in the light curve exhibits inflections. The duration between them is

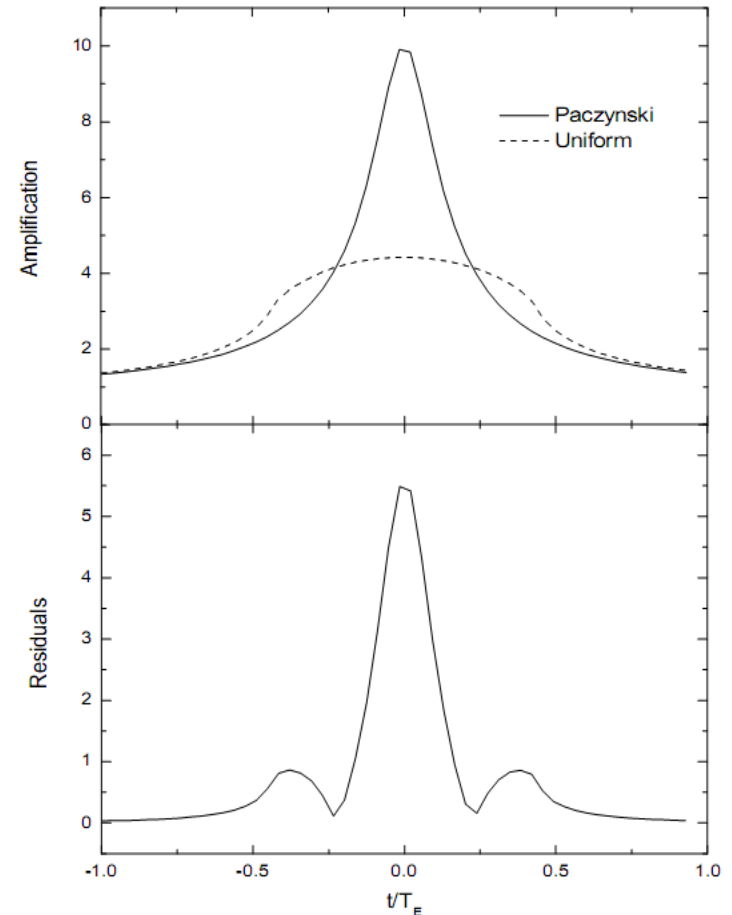
$$T = 2\sqrt{\rho_*^2 - u_0^2} T_E$$

By this relation can be defined  $\rho_*$

With the additional information about the angular source size  $\theta_*$ , can be define the angular Einstein radius by

$$\theta_E = \frac{\theta_*}{\rho_*}$$

Since  $\theta_E$  does not depend on  $v_T$ , the physical parameters of the lens can then be better constrained.



**Up.** The amplification of a microlensing event. The event parameters are:  $u_0 = 0.1$ ,  $\rho_* = 0.46$ ,  $T_E = 9.2\text{h}$ . The duration of the lens transit over the source disk turns out to be  $T \approx 0.9T_E \approx 8.2$  hours,

**Down.** The residuals between the two curves.

# The amplification of finite source effects

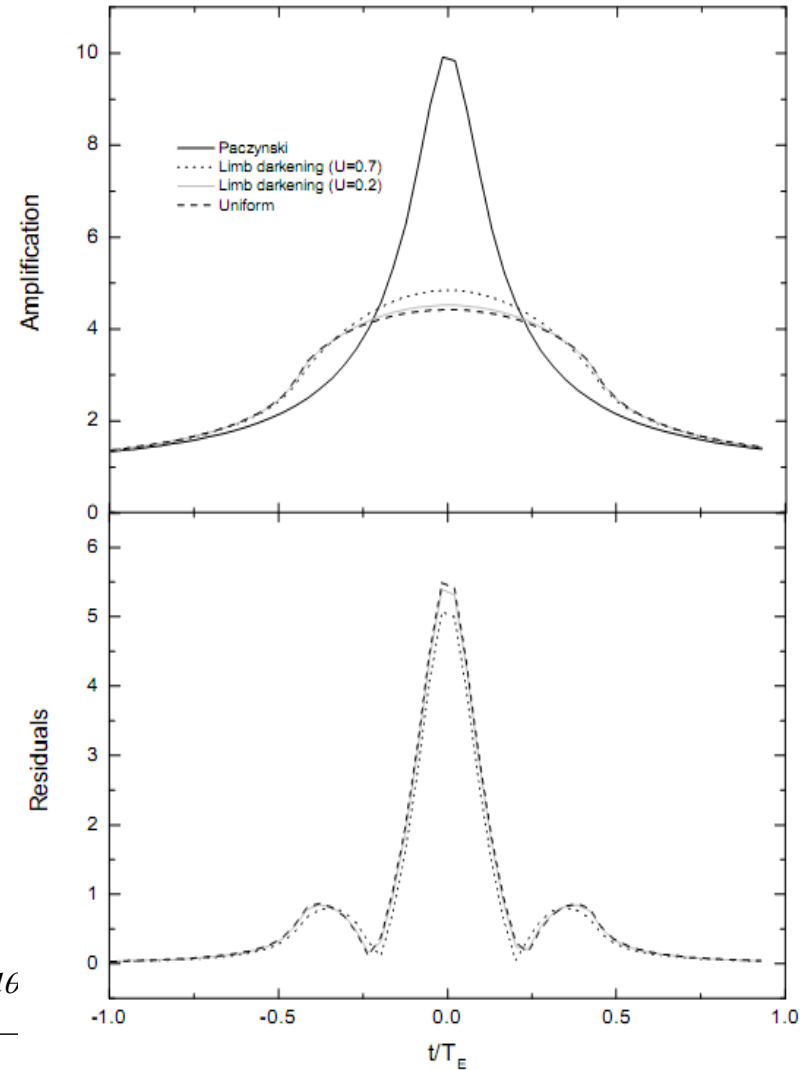
The amplification in light curve when the source brightness is uniform.

$$A_{fs}(u) = \frac{1}{\pi\rho_*^2} \int_0^{\rho_*} \int_0^{2\pi} A(u') r dr d\theta =$$

$$= \frac{1}{\pi\rho_*^2} \int_0^{\rho_*} \int_0^{2\pi} \frac{u^2 + r^2 - 2ur \cos \theta + 2}{\sqrt{u^2 + r^2 - 2ur \cos \theta} \sqrt{u^2 + r^2 - 2ur \cos \theta + 4}} r dr d\theta$$

The amplification in light curve when the source brightness is given by a linear limb-darkening profile,  $I(\mu) = I(1)[1 - U(1 - \mu)]$

$$A_{fs}(u) = \frac{\int_0^{\rho_*} \int_0^{2\pi} \frac{u^2 + r^2 - 2ur \cos \theta + 2}{\sqrt{u^2 + r^2 - 2ur \cos \theta} \sqrt{u^2 + r^2 - 2ur \cos \theta + 4}} [1 - U(1 - \sqrt{\frac{\rho_*^2 - r^2}{\rho_*^2}})] r dr d\theta}{2\pi \int_0^{\rho_*} [1 - U(1 - \sqrt{\frac{\rho_*^2 - r^2}{\rho_*^2}})] r dr}$$



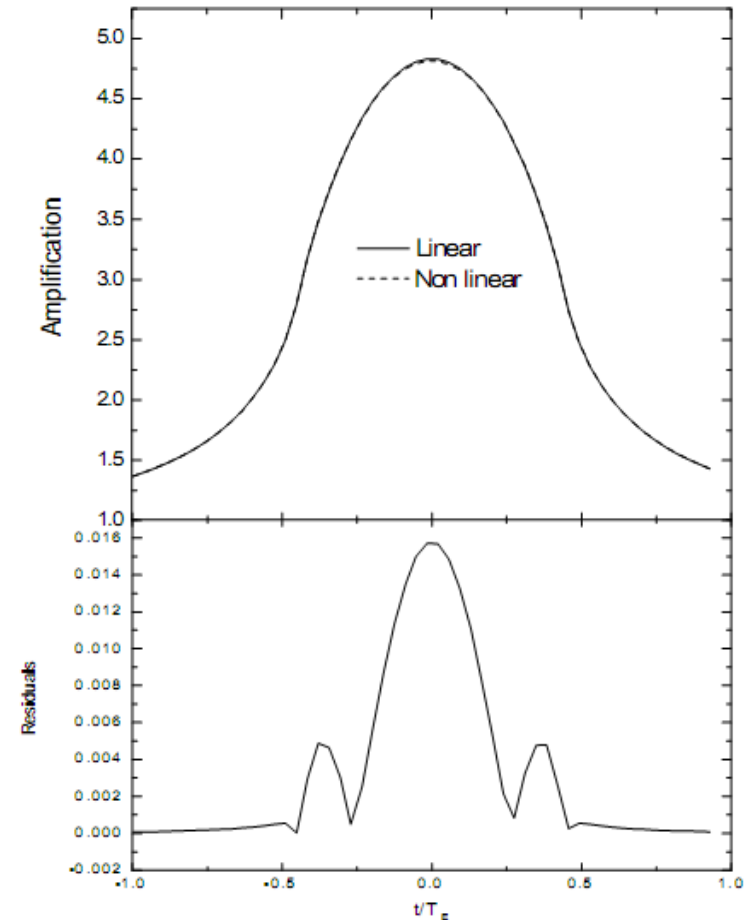
# Conditions of observing the finite source effects

A microlensing event will be detected if there are at least eight consecutive points with amplification bigger than  $A_{th}=1.001$ . Since the cadency is 20 min, the event have to a duration longer than 2.67 h to be detectable.

Since the photometric error of Euclid is 0.1% we find that the residuals between the standard and the finite source curve have to be  $Res=|A_s-A_{fs}|=0.001$ .

The finite source effects are detected when there are at least 8 points around the event peak in which  $Res > 0.001$

The residuals at the peak is up to 0.32%, so the different limb darkening profiles are distinguishable by Euclid.



**Up.** The amplification of a microlensing event ( $u_0 = 0.1$ ,  $\rho_* = 0.46$ ) for linear LDC ( $U = 0.6866$ ) and for four parameter non-linear power law ( $a1 = 0.7181$ ,  $a2 = -0.5941$ ,  $a3 = 1.1698$  and  $a4 = -0.4558$ ).

**Down.** The residuals between the two curves.

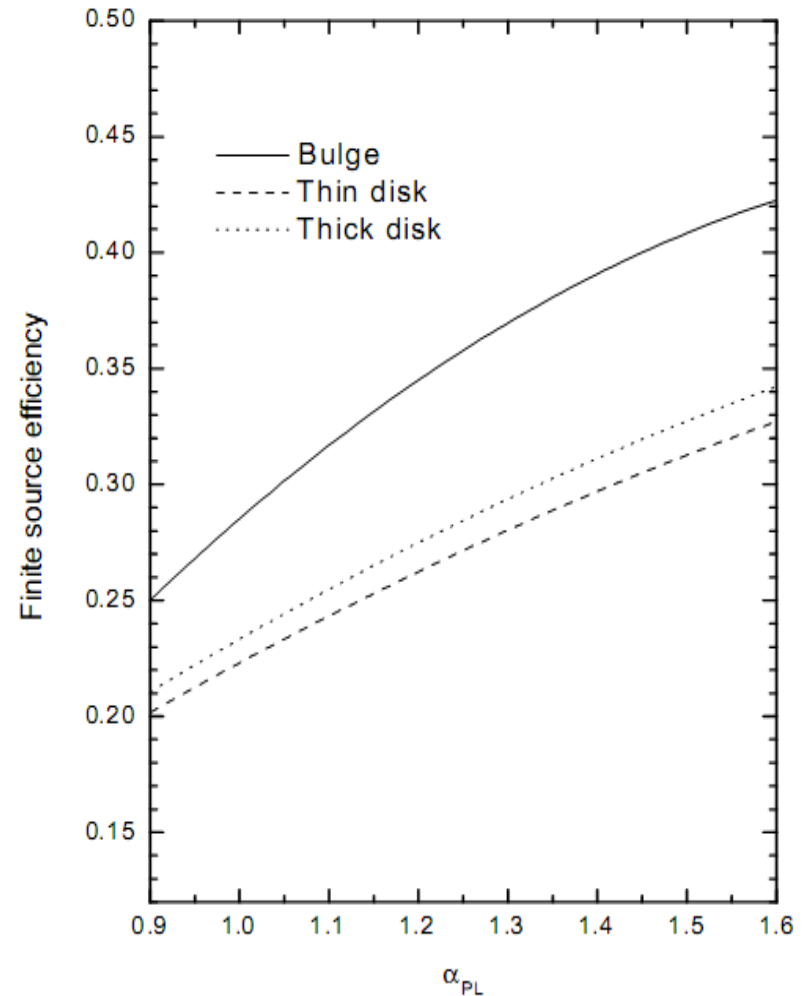
# Monte Carlo simulations

We begin by drawing:

- The FFP distance from Earth  $D_L$  is extracted based on the disk and bulge, FFP spatial distributions along the Euclid line of sight ( $b = 1.7^\circ$ ,  $l = 1.1^\circ$ ).
- The event impact parameter  $u_0$  is assumed to be uniformly distributed in the interval  $[0, 6.54]$ .
- The FFP relative transverse velocity is extracted from the velocity distribution
- The lens mass is assumed to follow the mass function.
- By the free code available in the web site <http://iac-star.iac.es> we generate a synthetic stellar population.
- We use the site <http://vizier.u-strasbg.fr/viz-bin/VizieR-3?source=J/A%2bA/363/1081/phoenix> to find the four LDCs:  $a_1$ ,  $a_2$ ,  $a_3$ ,  $a_4$  of non-linear law.
- The source distances  $D_S$ , based on the above written bulge spatial distributions, result to be in the range  $7 \div 10$  kpc.

# Efficiency of finite source effects

The efficiency for finite source effects is the ratio of the event's number with finite source effects with the total number of detectable events.

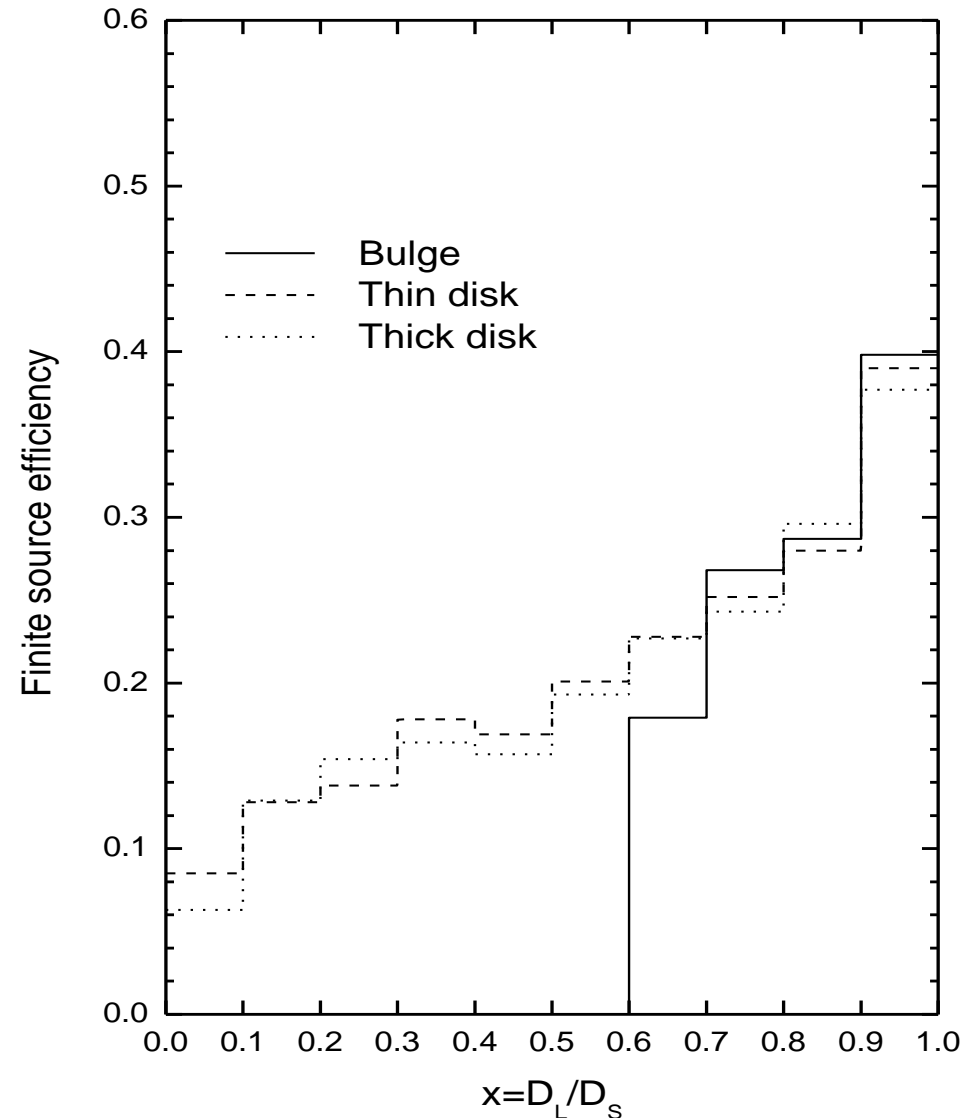




# Finite source efficiency versus $x$

Simulating 1000 microlensing events for each defined bin range  $[0; 0.1]$ – $[0.9; 1]$  and for  $\alpha_{\text{PL}} = 1.3$ , we calculate the finite source efficiency as defined above.

- The finite source efficiency increases with the  $x$  value.
- For FFPs in the thin and thick disks we note that the finite source efficiency slightly diminishes in the  $[0.4, 0.5]$  bin, because the  $R_E$  gets its maximum value at  $x = 0.5$ .



# Conclusions

- We emphasize that the Euclid program will offer the unique opportunity to detect the finite source effects in microlensing events caused by FFPs.
- Using Monte Carlo numerical simulations, we investigate that 1/3 of observable events will have finite source effect detected.
- Since Euclid will detect a considerably large number of events caused by FFPs, the events with detectable finite source effects will allow to constrain the FFP mass and distances, which is a fundamental information necessary to investigate for FFP populations through out the Milky Way.
- Also the high-magnification microlensing events caused by FFPs are the unique possibility to investigate the Galactic bulge star atmospheres, and to define the source limb-darkening profile.

# Bibliography

- **B. Paczyński, *Astrophys. J.* 304 (1986) 1**
- **H. J. Witt, *Astrophys. J.* 449 (1995) 42**
- **R. J. Nemiroff and W.A.D.T. Wickramasinghe, *Astrophys. J.* 424 (1994) 21**
- **J. Y. Choi et al., *Astrophys. J.* 751 (2012) 41**
- **J. A. Johnson, B. S.Gaudi, T. Sumi, I. A. Bond, and A. Gould *Astrophys. J.* 685 (2008) 508**
- **G. Ingrosso, S. Calchi Novati, F. De Paolis, Ph. Jetzer, A. A. Nucita, F. Strafella, A. F. Zakharov *MNRAS* 426 (2012) 1496**
- **G. Ingrosso, F. De Paolis, A. A. Nucita, F. Strafella, S. Calchi Novati, Ph. Jetzer, G. Liuzzi, A. F. Zakharov *Physica Scripta* 89(2014) 084001**
- **R. K. Peña et al., *Astrophys. J.* 754 (2012) 30**
- **L. Hamolli, M. Hafizi and A. Nucita, *Int. Journ. Mod. Phys. D* 22 (2013) No. 10**
- **T. Sumi, K. Kamiya, A. Udalski, D. Bennett, I. Bond *Nature* 473 (2012) 349**
- **G. Gilmore, R. F. G. Wyse, K. Kuijken, *Astron. Astrophys.* 27 (1989) 555**
- **F. De Paolis, G. Ingrosso and A. Nucita, *Astron. Astrophys.* 366 (2001) 1065**
- **M. Hafizi, F. De Paolis, G. Ingrosso and A. Nucita, *Int. Journ. Mod. Phys. D* 13 (2004) 1831**
- **E. Dwek, R. G. Arendt, M. G. Hauser *Astrophys. J.* 445 (1995) 716**
- **Ch. Han and A. Gould, *Astrophys. J.* 447 (1995) 53**
- **Ch. Han et al., *Astrophys. J.* 604 (2004) 372**
- **E.A. Milne, *MNRAS* 81 (1921) 361**
- **D. A. Klingsmith and S. Sobiesky, *Astrophys. J.* 75 (1970) 175**
- **A. Claret and A. Giménez, *Astron. Astrophys.* 230 (1990) 412**
- **W. Van Hamme, *Astrophys. J.* 106 (1993) 2096**
- **A. Manduca, R. A. Bell and B. Gustafsson, *Astron. Astrophys.* 61 (1977) 809**
- **J. Díaz-Cordovés and A. Giménez, *Astron. Astrophys.* 259 (1992) 227**
- **A. Claret, *Astron. Astrophys.* 363 (2000) 1081**
- **S. Rahvar and M. Dominik, *MNRAS* 392 (2009) 1193**
- **A. Aparicio and C. Gallart *Astrophys. J.* 128 (2004) 1465**

Faleminderit